

Fast Terminal Sliding Mode Control for the Soft Landing of a Space Robot on an Asteroid Considering a Barycentric Gravitational Model

Mahsa Azadmanesh¹, Jafar Roshanian², Mostafa Hassanalian³,

1,2- *K.N.Toosi University of Technology*, Tehran, Iran.

3- *New Mexico Tech University*, Socorro, New Mexico, US.

Abstract

This study aims to control a space robot's soft-landing trajectory on the asteroid EROS433 considering a weak, yet effective gravitational field. As the research innovation, the study employs a fast terminal sliding mode control (FTSMC) to manage the landing trajectory and enhance the dynamic tracking performance for the soft landing of the space robot on the asteroid. This controller can ensure that the system modes are positioned on the sliding surface within a limited time. As an advantage over the PD sliding mode controller, the proposed controller raises the speed and improves the accuracy of tracking the desired trajectory and enhances the robustness of the control system. The study further compares the results of simulations performed in MATLAB to evaluate the proposed controller design.

Keywords: *Space Robot Landing, Fast Terminal Sliding Mode Control, Asteroid, Lyapunov Stability.*

1. Introduction

Small planetary bodies such as asteroids and comets are of high scientific interest, as the properties of their organic substance are possible targets for future explorations on the origins of life. Besides, these objects may pose an impact hazard on the planet Earth [1-4].

Soft landing on asteroids is amongst the most challenging tasks in deep space exploration. In the soft-landing process, the space robot must reach superior fuel performance during the decline stage and ensure an accurate soft landing. In order to guarantee a safe and successful space robot landing on asteroids, it is crucial to control and adjust the trajectory and velocity of the space robot in real time [5].

Ref. [6] proposed a novel sliding mode-fuzzy control approach to achieve the soft landing according to the nominal trajectory. The study employed fuzzy rules to gain better control of the airship for tuning switching control and using adaptation law to compensate for model uncertainties of the airship.

Ref. [7] divided landing control into velocity control and control over velocity decline rate and proposed a proportional navigation (PN) guidance law with a final condition and a velocity-decline-rate-control law.

Ref. [8] proposed an orbital maneuver strategy based on piecewise linear optimization for spacecraft's soft landing on irregular asteroids. In this study, the space around an irregular asteroid was first converted into several grid units, and the asteroid's gravitational field was linearly fitted in each unit. The study then formulated the soft-landing orbital maneuver strategy design problem as a piecewise linear optimal problem. It further changed the problem into a family of two-point boundary value problems, which can be solved using the collocation method. A corresponding algorithm was eventually developed to achieve the piecewise linear optimal maneuver strategy, which efficiently accomplished the soft-landing mission. According to the simulation results, the model linearization error was negligible, while the calculation efficiency and the robustness of the maneuver strategy were significantly improved.

In Ref. [9], an autonomous navigation strategy was proposed to achieve fast-tracking by employing the sliding mode variable structure control (SMVSC) method.

Ref. [10] proposed a nonlinear-optimal-control-law design based on a neuro-fuzzy system to track the optimal landing trajectory on the moon.

Ref. [11] used a fuzzy-variable structure control (VSC) approach to guide the spacecraft's final landing trajectory on the moon. The control approach is more robust than linearization-based dynamic methods. However, landing on an asteroid is more complicated than landing on the moon, as asteroids are irregular in shape and have a sharp rotary shaft and a rough surface. Hence, it is crucial to improve the proposed strategy to allow the soft landing of the probe on asteroids.

Ref. [12] employed the nonsingular terminal sliding mode (NTSM) control technique to address the finite-time soft-landing problem of an asteroid probe. The study formulated the problem as a two-point boundary-value constraints control problem, including all the initial and terminal requirements of the soft-landing problem. Then, it proposed an NTSM control law for a soft landing on an asteroid concerning the specific characteristics of the problem. According to the

1. PhD Candidate, *Faculty of Aerospace Engineering*, mahsa.azadmanesh@yahoo.com (corresponding author)

2. Professor, *Faculty of Aerospace Engineering*, roshanian@kntu.ac.ir

3. Assistant professor, *Mechanical Engineering Department*, mostafa.hassanalian@nmt.edu

simulation results, the proposed method provided a much faster convergence rate, higher accuracy, better disturbance rejection properties, and stronger robustness against the parameter uncertainties compared to the typical traditional sliding mode control method.

Ref. [13] proposed a novel nonlinear guidance algorithm for a spacecraft hovering and landing on asteroids. The proposed guidance allowed the spacecraft to achieve its target position and velocity in finite time without reference trajectories. The study performed a parametric analysis to describe the parameters' effects on the guidance algorithm. It further presented a straight landing simulation, hovering and landing on the irregular asteroid 2063 Bacchus, and the effectiveness of the proposed method was established.

Most studies on the space robot (probe) soft landing tasks simulated the asteroid by a three-axis ellipsoid model, whose gravitational potential is expressed as a spherical second-order harmonic expansion. However, for an asteroid with a weak gravitational field due to its irregular shape and uneven mass distribution, this model comes with high inaccuracies. Accordingly, this study aims to design a fast terminal SMC (FTSMC) to fast track the desired trajectory based on a barycentric gravity model with two more accurate mass centers.

2. Dynamic Equations for a Space Robot Landing on an Asteroid

Fig. 1 illustrates a space robot or a probe sampling (landing) on an asteroid. The dynamic equations of the robot in the fixed-body coordinate system are as follows [5],



Fig. 1. A probe landing on the asteroid [14].

$$\begin{cases} \ddot{x} - 2\omega\dot{y} - \omega^2x = g_x + u_x + D_x \\ \ddot{y} + 2\omega\dot{x} - \omega^2y = g_y + u_y + D_y \\ \ddot{z} = g_z + u_z + D_z \end{cases} \quad (1)$$

where $\omega = 3.3118 \times 10^{-4}$ is the angular speed of the rotation of asteroid EROS433, x , y , and z are components of the position vector of the space robot in the fixed-body coordinate system, $[u_x \ u_y \ u_z]$ is the relative control acceleration vector along the three axes, and D_x , D_y , and D_z are the sum of the modeling uncertainties along each axis. $[g_x \ g_y \ g_z]$ is the point gravitation vector with two mass centers along the three axes and is obtained as follows [15, 16],

$$\begin{cases} U = G \left(\frac{M_1}{\sqrt{(x-x_1)^2 + (y-y_1)^2 + (z-z_1)^2}} + \frac{M_2}{\sqrt{(x-x_2)^2 + (y-y_2)^2 + (z-z_2)^2}} \right) \\ g_x = \frac{\partial U}{\partial x} = \left(\frac{GM_1(x-x_1)}{((x-x_1)^2 + (y-y_1)^2 + (z-z_1)^2)^{1.5}} + \frac{GM_2(x-x_2)}{((x-x_2)^2 + (y-y_2)^2 + (z-z_2)^2)^{1.5}} \right) \\ g_y = \frac{\partial U}{\partial y} = \left(\frac{GM_1(y-y_1)}{((x-x_1)^2 + (y-y_1)^2 + (z-z_1)^2)^{1.5}} + \frac{GM_2(y-y_2)}{((x-x_2)^2 + (y-y_2)^2 + (z-z_2)^2)^{1.5}} \right) \\ g_z = \frac{\partial U}{\partial z} = \left(\frac{GM_1(z-z_1)}{((x-x_1)^2 + (y-y_1)^2 + (z-z_1)^2)^{1.5}} + \frac{GM_2(z-z_2)}{((x-x_2)^2 + (y-y_2)^2 + (z-z_2)^2)^{1.5}} \right) \end{cases} \quad (2)$$

where U is the gravitational potential function of the asteroid, G is the global gravitation constant, M_1 and M_2 are mass points of the asteroid, and (x_1, y_1, z_1) and (x_2, y_2, z_2) are the coordinates of the asteroid mass points (Fig. 2).

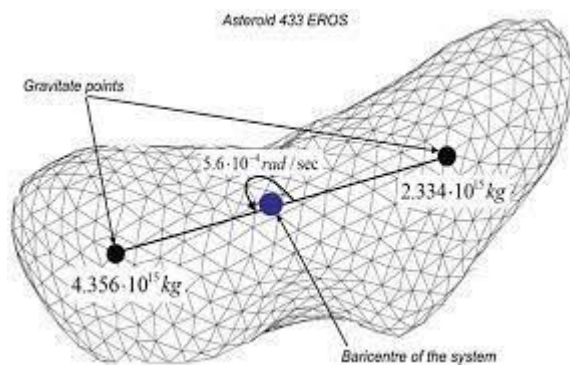


Fig. 2. Mass points of the asteroid EROS433 [16]

3. State-Space Equations

By considering the equations below

$$\begin{cases} X = [x_1 & x_2 & x_3 & x_4 & x_5 & x_6]^T = \\ & [x & \dot{x} & y & \dot{y} & z & \dot{z}]^T \\ & u = [u_x & u_y & u_z]^T \end{cases} \quad (3)$$

where X is the state-space vector and u is the vector of control inputs, the state-space form of Eq. (1) is converted into the following equation.

$$\begin{aligned} \dot{x}_1 &= x_2 \\ \dot{x}_2 &= 2\omega x_4 + \omega^2 x_1 + g_x + u_x + D_x \\ \dot{x}_3 &= x_4 \\ \dot{x}_4 &= -2\omega x_2 + \omega^2 x_3 + g_y + u_y + D_y \\ \dot{x}_5 &= x_6 \\ \dot{x}_6 &= g_z + u_z + D_z \end{aligned} \quad (4)$$

4. Fast Terminal Sliding Mode Control (FTSMC)

The sliding-mode control approaches the problem of consistent performance systematically in a way that the response remains insensitive to the uncertainties and disturbances [17].

Fast terminal sliding mood control (FTSMC) for landing along with the x -direction using the sliding surface is defined as follows,

$$s_1 = \dot{e}_{1x} + \beta(e_{1x})^{\frac{p}{q}} \quad (5)$$

where $e_{1x} = x_1 - x_d$ and x_d is the optimal landing trajectory for the x -axis (Table 1). In addition, β is a positive parameter, and p and q ($p < q$) are integers. Including the nonlinear term $(e_{1x})^{p/q}$ results in convergence in finite time $t_s = \left(\frac{p}{\beta(p-q)}\right) |e_1(0)|^{\frac{p-q}{p}}$ to the origin. Thus, using parameters β , p and q allows for adjusting the convergence time. A drawback of the above sliding surface is that the convergence time depends on the initial distance from the sliding surface, in which, by increasing the distance, the convergence time is increased proportional to $|e_1(0)|^{\frac{p-q}{p}}$. To address this problem, FTSMC is proposed as follows [18-23],

$$s_1 = \dot{e}_{1x} + \alpha e_{1x} + \beta(e_{1x})^{\frac{p}{q}} \quad (6)$$

where α is a positive parameter. Now, it must be clarified how the sliding surface reduces the convergence time. If the system states are on the sliding surface, then the equation $\dot{e}_{1x} = -\alpha e_{1x} - \beta(e_{1x})^{p/q}$ is established. When the initial state is far away from the origin, the approximate dynamic will be as $\dot{e}_{1x} = -\alpha e_{1x}$. On the contrary, when the initial state is adjacent to the origin, the approximate dynamic is $\dot{e}_{1x} = -\beta(e_{1x})^{p/q}$. Now, using parameters α and β , the convergence time can be adjusted independently for far and near distances. The convergence time can be obtained from the equation below [18].

$$t_s = \frac{p}{\alpha(p-q)} \left(\ln \left(\alpha e_1^{\frac{p-q}{p}} + \beta \right) - \ln \beta \right) \quad (7)$$

5. Control Input Design and Stability Analysis

5.1. Optimal Trajectory Design

The design of the nominal properties of the trajectory enabled the space robot to reach the specified landing location in a certain amount of time and within all the landing limitations. For a safe landing on an asteroid, the vertical speed should be low enough to prevent the space robot from overturning or being damaged [5]. Here, the landing trajectory was assumed as a third-degree polynomial for fall planning, as Eq. (8) describes.

$$x_d(t) = x_0 + x_1 t + x_2 t^2 + x_3 t^3 \quad (8)$$

The following four equations were considered to find the unknown x_0 , x_1 , x_2 , and x_3 according to Table 1.

$$\begin{cases} x_d(0) = 3200 \Rightarrow x_0 = 3200 \\ \dot{x}_d(0) = -1.2 \Rightarrow x_1 = -1.2 \\ x_d(8000) = 2837 \\ \dot{x}_d(8000) = 0 \end{cases} \Rightarrow \begin{cases} x_2 = 2.83 \times 10^{-4} \\ x_3 = -1.73 \times 10^{-8} \end{cases} \quad (9)$$

Similarly, considering the fact that the final time was $t = 8000$ s, the landing trajectory of variables y and z were calculated.

$$\begin{cases} y_d(t) = 1300 + \\ 0.2t - 6.74 \times 10^{-5} t^2 + 4.58 \times 10^{-9} t^3 \\ z_d(t) = 9000 - \\ t + 9.57 \times 10^{-5} t^2 - 2.76 \times 10^{-9} t^3 \end{cases} \quad (10)$$

Since the procedure was similar for all three state variables, the input design procedure was only followed for state variable X .

5.2. Control Input Design

Considering the values of simulation parameters for space robot landing, the state vectors of positions, and optimal velocities listed in Table 1, the derivation of Eq. (6) led to the following equation.

$$\dot{S}_1(x) = \ddot{e}_{1x} + \dot{e}_{1x} \left(\alpha + \beta \frac{p}{q} (e_{1x})^{\frac{p}{q}-1} \right) \quad (11)$$

TABLE I. THE SIMULATION VARIABLES OF THE SPACE ROBOT LANDING ON ASTEROID EROS433 [5]

Variable	Value	Unit
Optimal	[3200	
Initial	1300	m
Position	9000]	

Optimal Initial Speed	[-1.2 0.2 -1]	m/s
Landing Position	[2837 928.1 5708]	m
Optimal Final Speed	[0 0 0]	m/s
Average Asteroid Weight	6.69×10 ⁵	kg
Space Robot Weight	150	kg
Average Asteroid Radius	16000	m
Gravitational Constant	6.6743×10 ⁻¹¹	m ² kg ⁻¹ s ⁻²

Since the sliding surface equation was defined based on state variables and the optimal position, the system would converge to the optimal position on the sliding surface. So, the following equation holds for the sliding surface.

$$\begin{cases} s_1 = 0 \\ \dot{s}_1 = 0 \end{cases} \quad (12)$$

Regarding the sliding mode theory, control input u_x is defined as [24,25]

$$u_x = u_{xeq} + u_{xs} \quad (13)$$

where u_{xeq} is the equivalent control component keeping the states on the sliding surface, and u_{xs} is the switching component driving the states towards the sliding surface. In fact, u_{xs} is the system stabilizer, determined by the Lyapunov stability.

The equivalent control component (u_{xeq}) is calculated by setting $\dot{s}_1 = 0$.

$$\begin{aligned} \dot{s}_1(x) &= \ddot{e}_{1x} + \dot{e}_{1x} \left(\alpha + \beta \frac{p}{q} (e_{1x})^{\frac{p-1}{q}} \right) = 0 \\ &\Rightarrow (\dot{x}_2 - \dot{x}_{2d}) \\ &\quad + (x_2 - x_{2d}) \left(\alpha + \beta \frac{p}{q} (e_{1x})^{\frac{p-1}{q}} \right) = 0 \\ &\Rightarrow u_{1eq} \\ &= -(2\omega x_4 + \omega^2 x_1 + g_x + D_x - \dot{x}_{2d}) \\ &\quad - (x_2 - x_{2d}) \left(\alpha + \beta \frac{p}{q} (e_{1x})^{\frac{p-1}{q}} \right) \end{aligned} \quad (14)$$

The Lyapunov candidate function is assumed to be a definite positive function defined below.

$$V_1 = \frac{1}{2} s_1^2 > 0 \quad (15)$$

For asymptotic stability, the derivation of Eq. (15) should be a definite negative value.

$$\begin{aligned} \dot{V}_1 &= s_1 \dot{s}_1 = s_1 \left(\ddot{e}_1 + \dot{e}_1 \left(\alpha + \beta \frac{p}{q} (e_1)^{\frac{p-1}{q}} \right) \right) \\ &= s_1 \left((\dot{x}_2 - \dot{x}_{2d}) \right. \\ &\quad \left. + (x_2 - x_{2d}) \left(\alpha + \beta \frac{p}{q} (e_{1x})^{\frac{p-1}{q}} \right) \right) \\ &= s_1 \left(2\omega x_4 + \omega^2 x_1 + g_x + (u_{xeq} + u_{xs}) + D_x - \dot{x}_{2d} \right. \\ &\quad \left. + (x_2 - x_{2d}) \left(\alpha + \beta \frac{p}{q} (e_{1x})^{\frac{p-1}{q}} \right) \right) < 0 \end{aligned} \quad (16)$$

Using Eq. (14) and substituting in Eq. (16),

$$\dot{V}_1 = s_1(u_{xs}) < 0 \quad (17)$$

Thus, a candidate for switching control rules that can satisfy Eq. (17) is

$$u_{xs} = -k_1 \text{sgn}(s_1) \quad (18)$$

where k_1 is a real positive parameter. Combining Eqs. (14) and (18), and substituting in Eq. (13), the general equation of FTSM to use for tracking the space robot's reference trajectory is given by Eq. (19).

$$\begin{aligned} u_x &= -(2\omega x_4 + \omega^2 x_1 + g_x + D_x - \dot{x}_{2d}) \\ &\quad - (x_2 - x_{2d}) \left(\alpha + \beta \frac{p}{q} (e_{1x})^{\frac{p-1}{q}} \right) \\ &\quad - k_1 \text{sgn}(s_1) \end{aligned} \quad (19)$$

This paper evaluated the space robot system by employing an FTSM strategy in two cases using MATLAB. For the first case, the sign function was adopted, and for the second one, the sign function was replaced by a saturation function in the switching input, and an uncertainty was applied to the system at the speed of EROS433 rotation.

6. MATLAB Simulations

6.1. Fast Terminal Sliding Mode Control with a Sign Function

By setting the simulation time (T_{sim}) to 15 s and the sampling time constant (T_s) to 0.01, and regarding the values presented in Table 1, the control inputs designed

in section 5 for all Cartesian coordinates were implemented in MATLAB, and the following graphs were derived.

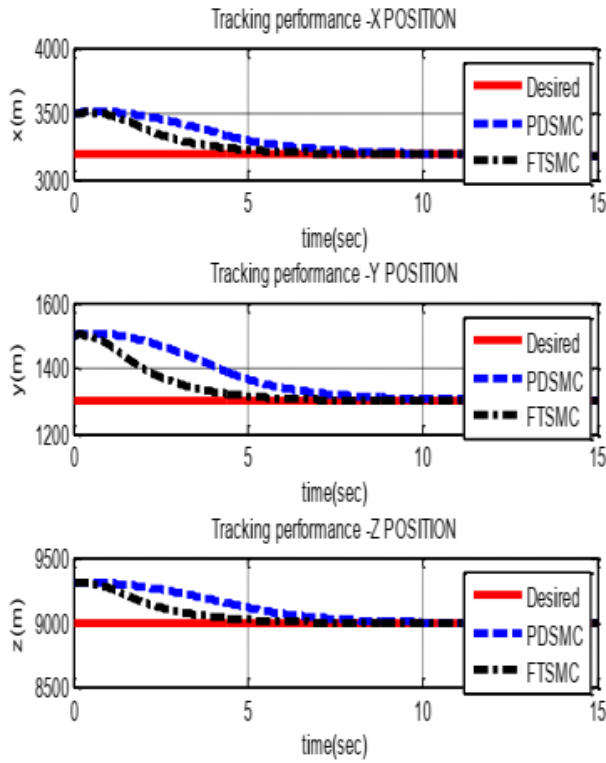


Fig. 3. The tracking performance of the desired space robot trajectory with a classic PD sliding mode and fast terminal mode with a sign function

Regarding Fig. 3, FTSMC was able to track the optimal space robot trajectory in a shorter period than the classic PD sliding mode control.

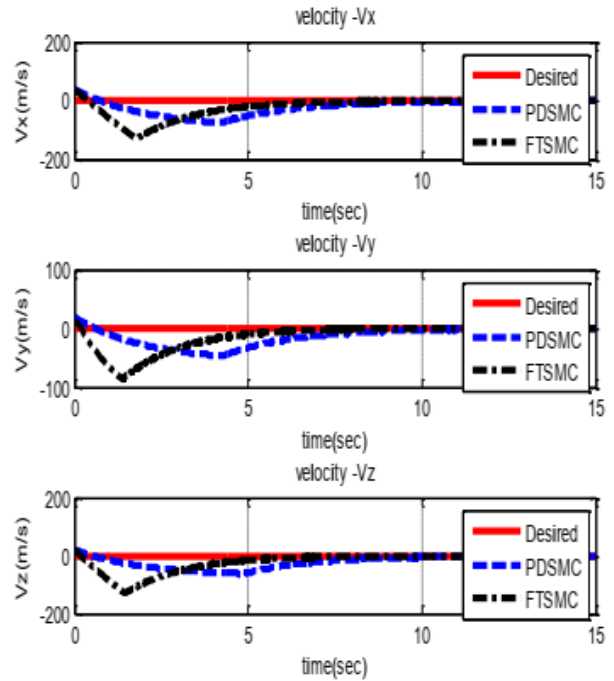


Fig. 4. The space robot optimal velocity tracking with a classic PD sliding mode and fast terminal mode with a sign function

Fig. 4 illustrates that FTSMC could track the optimal space robot speed faster than the classic PD sliding mode control.

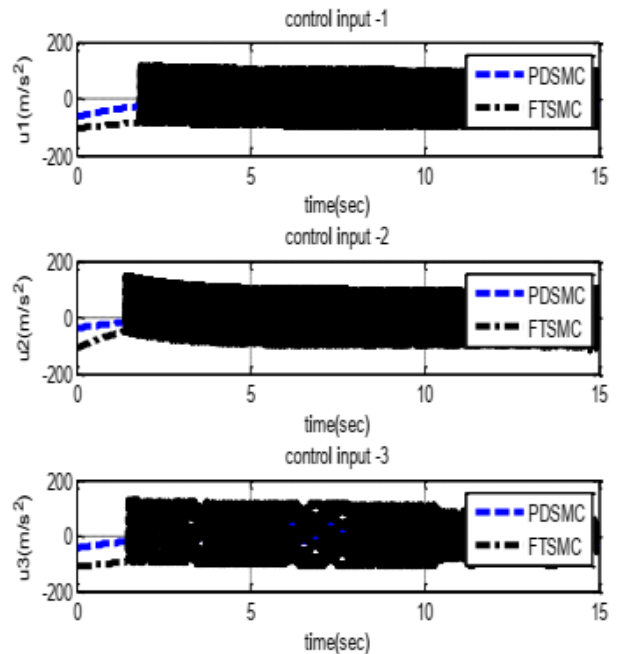


Fig. 5. The control attempt with a classic PD sliding mode and fast terminal mode with a sign function

Some parasitic oscillation (chattering) was observed in Fig. 5 due to the states' derivatives. This is explained in the following.

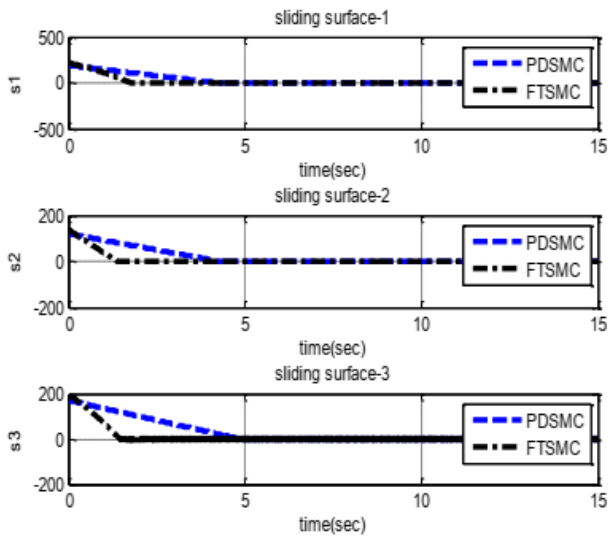


Fig. 6. Sliding surface to control with a classic PD sliding mode and fast terminal mode with a sign function

Fig. 6 shows that FTSMC could converge and stabilize the sliding surface faster than the classic PD sliding mode control.

Evaluation of Figs. 4-6, and the control phase revealed that the trajectories along all three coordinate axes were tracked in less than 5 s, which is acceptable, while this was done in about 8 s using the classic PD sliding mode control. So, short solution time is a major advantage of FTSMCs. There were some oscillations, especially in control inputs, because they dealt with derivatives and amplified the high-frequency components.

6.2. Fast Terminal Sliding Mode Control with a Hyperbolic Tangent Function

By setting $T_{sim} = 15$ s, $T_s = 0.01$, adopting the smooth hyperbolic tangent as the control function, and regarding the values presented in Table 1, the control inputs designed in section 5 for all Cartesian coordinates were implemented in MATLAB, and the following graphs were derived.

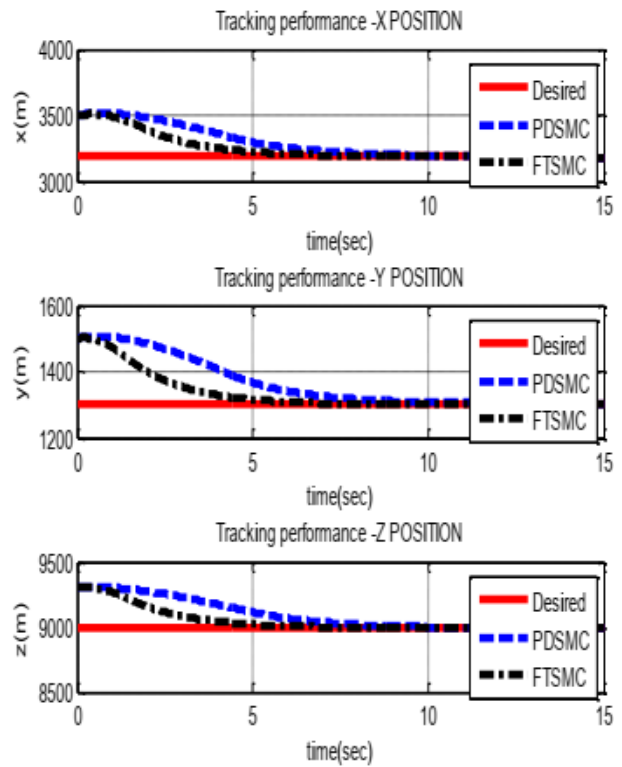


Fig. 7. Tracking the desired trajectory of the space robot with classic PD sliding mode and fast terminal mode with a hyperbolic tangent function

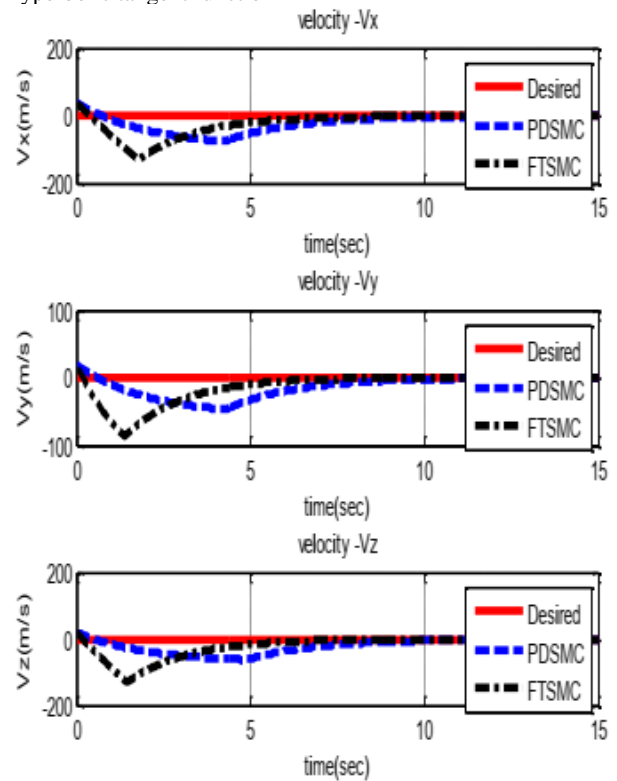


Fig. 8. Tracking the optimal trajectory of the space robot with classic PD sliding mode and fast terminal mode with a hyperbolic tangent function

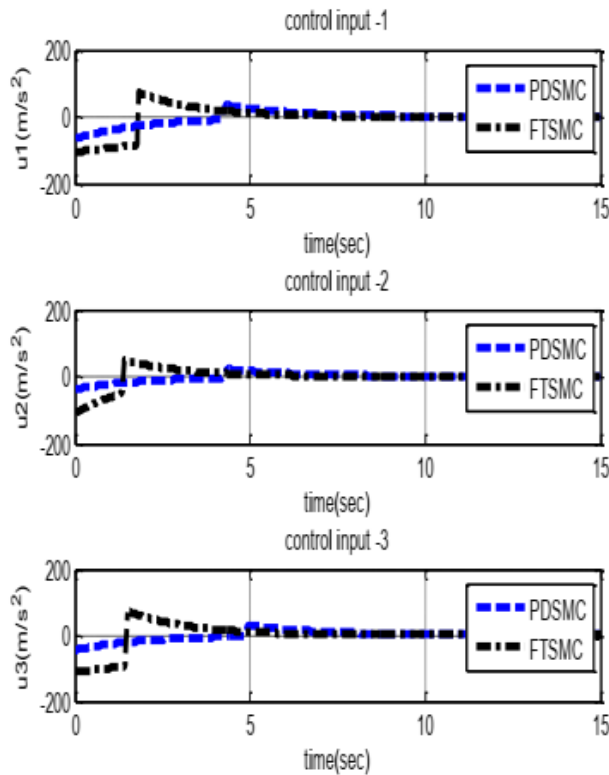


Fig. 9. The control attempt with PDCMC and FTSMC modes with a hyperbolic tangent function

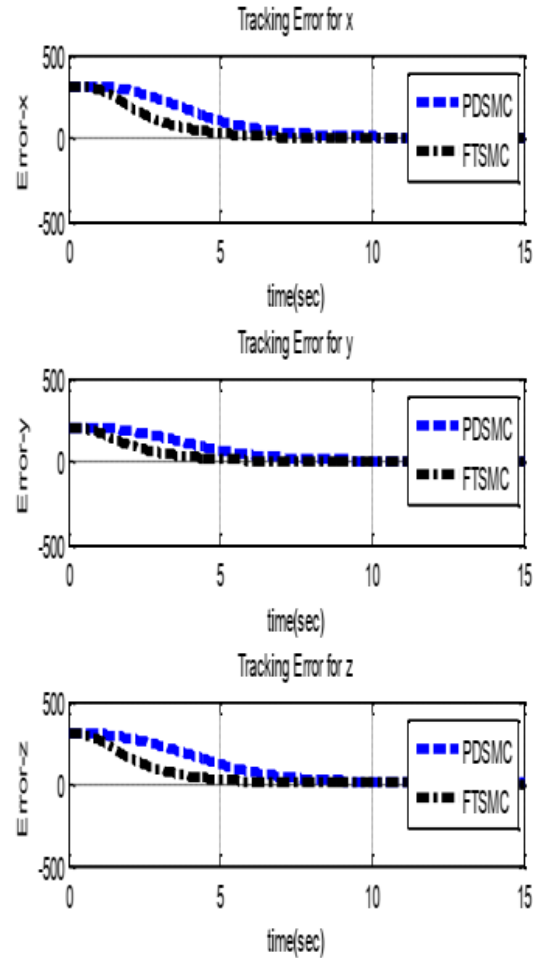


Fig. 10. Location tracking error for three moving axes with PDCMC and FTSMC modes with a hyperbolic tangent function

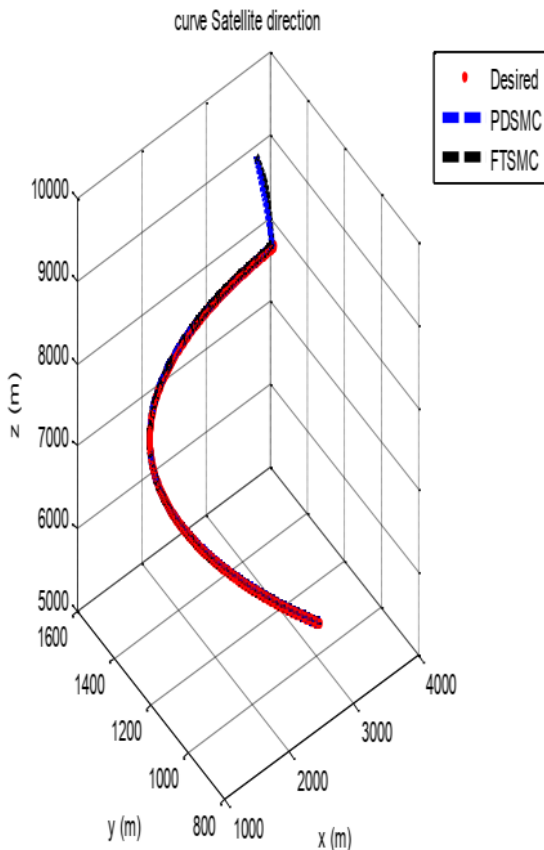
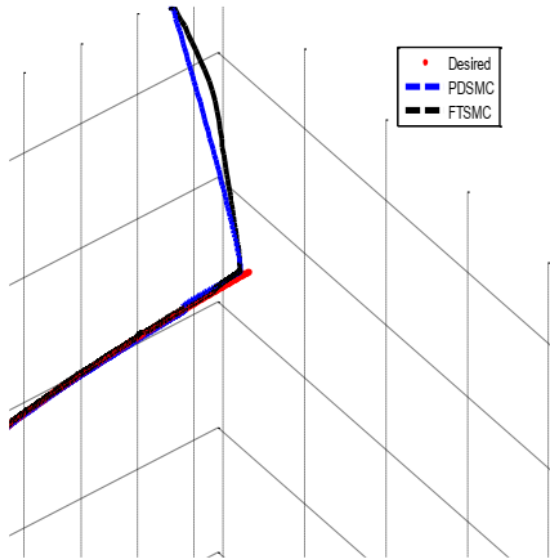


Fig. 11. Location tracking error for three moving axes with PDCMC and FTSMC modes with a hyperbolic tangent function

Figs. 7-10 show that the trajectory tracking was conducted more smoothly due to the inherent characteristics of saturation functions such as hyperbolic tangent. However, the convergence rate might be a little higher than the previous one in some

cases. Hence, the oscillations of states and control input were completely eliminated in Fig. 9. As shown in Fig. 10, the position tracking error tended to be zero, and the tracking had an efficient accuracy, with FTSMC being more accurate than classic PD sliding mode.

Table 2 reports the total error for both controllers.

TABLE II. THE ABSOLUTE ERROR FOR FTSMC AND PD SLIDING MODE CONTROLLER

Controller	Value
Fast Terminal Sliding Mode Controller	139/6112
Proportional-Derivative Sliding Mode Controller	244/8155

It can be seen that the absolute error value for FTSMC was significantly lower than the PD sliding mode controller.

Fig. 10 shows the 3D trajectory of the space robot from the beginning ($t = 0$) to the end ($t = 8000$ s), based on the optimal trajectory tracking. Firstly, it can be observed that the tracking was very fast and accurate. Secondly, the FTSMC outperformed the PD sliding mode controller.

The results indicated that chattering had a more profound effect on states' derivatives (e.g., control inputs).

Regarding the following Fourier transformation,

$$\frac{d}{dt}x(t) \overset{F}{\leftrightarrow} j\omega X(j\omega) \quad (20)$$

Eq. (20) suggests that time derivation leads to the linear amplification of system frequencies, meaning that higher frequencies were more severely amplified and low frequencies did not experience any significant changes. This results in the amplification of high-frequency components of the signals, for instance, obviously shown in Fig. 4.

7. Conclusions

This paper modeled the space robot landing system on asteroid EROS433. Then, the sliding surfaces, control inputs, a fast terminal sliding mode controller, and a proportional-derivative sliding mode controller were designed for the system. The controllers were simulated in MATLAB to be evaluated regarding their performance, and the results were satisfying. Sliding mode controllers are among the most prevalent

controllers of nonlinear systems and processes. Their popularity is due to their relative simplicity and resistance to system uncertainties and external perturbations. However, they have the disadvantage of state sliding on the sliding surface (chattering phenomenon), which is more significant in rapid dynamics systems. As discussed before, the sign function is replaced by a hyperbolic tangent to make the system behavior smoother and reduce the oscillations.

8. References

- [1] Yoshimitsu, Tetsuo, et al. "Micro-hopping robot for asteroid exploration." *Acta Astronautica* 52.2-6 (2003): 441-446.
- [2] Ulamec, Stephan, et al. "Landing on small bodies: From the Rosetta Lander to MASCOT and beyond." *Acta Astronautica* 93 (2014): 460-466.
- [3] Zhang, Tao, et al. "Drilling, sampling, and sample-handling system for China's asteroid exploration mission." *Acta Astronautica* 137 (2017): 192-204.
- [4] Tsuda, Yuichi, et al. "Hayabusa2 mission status: Landing, roving and cratering on asteroid Ryugu." *Acta Astronautica* 171 (2020): 42-54.
- [5] Li, Yuanchun, He Wang, Bo Zhao, and Keping Liu. "Adaptive fuzzy sliding mode control for the probe soft landing on the asteroids with weak gravitational field." *Mathematical Problems in Engineering* 2015 (2015). <https://doi.org/10.1155/2015/582948>
- [6] Yang, Yue-neng, Jie Wu, and Wei Zheng. "Trajectory tracking for an autonomous airship using fuzzy adaptive sliding mode control." *Journal of Zhejiang University SCIENCE C* 13, no. 7 (2012): 534-543. <https://doi.org/10.1631/jzus.C1100371>
- [7] Cui, H. T., X. Y. Shi, and P. Y. Cui. "Guidance and control law for soft landing asteroid." *Journal of Flight Dynamics* 20 (2002): 35-38. <https://doi.org/10.15982/j.issn.2095-7777.2019.02.010>
- [8] Zhiwei, H. A. O., Z. H. A. O. Yi, C. H. E. N. Ying, and Qihua Zhang. "Orbital maneuver strategy design based on piecewise linear optimization for spacecraft soft landing on irregular asteroids." *Chinese Journal of Aeronautics* 33, no. 10 (2020): 2694-2706. <https://doi.org/10.1016/j.cja.2019.12.011>
- [9] Cui, P. Y., S. Y. Zhu, and H. T. Cui. "Autonomous impulse maneuver control method for soft landing on small bodies." *Journal of Astronautics* 29, no. 2 (2008): 511-516. <https://doi.org/10.15982/j.issn.2095-7777.2019.02.010>
- [10] Zexu, Zhang, Wang Weidong, Li Litao, Huang Xiangyu, Cui Hutao, Li Shuang, and Cui Pingyuan. "Robust sliding mode guidance and control for soft landing on small bodies." *Journal of the Franklin Institute* 349, no. 2 (2012): 493-509. <https://doi.org/10.1016/j.jfranklin.2011.07.007>
- [11] Carson, John, Behcet Acikmese, Richard Murray, and Douglas MacMynowski. "Robust model predictive control with a safety mode: applied to small-body proximity operations." In *AIAA Guidance, Navigation and Control Conference and Exhibit*, p. 7243. 2008. <https://doi.org/10.2514/6.2008-7243>
- [12] Lan, Qixun, Shihua Li, Jun Yang, and Lei Guo. "Finite-time soft landing on asteroids using nonsingular terminal sliding mode control." *Transactions of the Institute of Measurement and Control* 36, no. 2 (2014): 216-223. <https://doi.org/10.1177%2F0142331213495040>
- [13] Yang, Hongwei, Xiaoli Bai, and Hexi Baoyin. "Finite-time control for asteroid hovering and landing via terminal sliding-mode guidance." *Acta Astronautica* 132 (2017): 78-89. <https://doi.org/10.1016/j.actaastro.2016.12.012>
- [14] Hilmi, Z. E. N. K., Halil ŞENOL, and Faruk GÜNER. "Lunar Excursion Module Landing Control System Design with P, PI and PID Controllers." *Karadeniz Fen Bilimleri Dergisi* 9, no. 2 (2019): 390-405. <https://doi.org/10.31466/kfbd.647211>
- [15] Shornikov, Andrei, and Olga Starinova. "Simulation of controlled motion in an irregular gravitational field for an electric propulsion spacecraft." In *2015 7th International Conference on Recent Advances in Space Technologies (RAST)*, pp. 771-776. IEEE, 2015. <https://doi.org/10.1109/RAST.2015.7208444>
- [16] Shornikov, Andrey, and Olga Starinova. "Boundary problem solution algorithm for the task of controlled spacecraft motion in irregular gravitational field of an asteroid." *Procedia engineering* 185 (2017): 411-417. <https://doi.org/10.1016/j.proeng.2017.03.323>
- [17] Ebrahimi, Behrouz, Mohsen Bahrani, and Jafar Roshanian. "Optimal sliding-mode guidance with terminal velocity constraint for fixed-interval propulsive maneuvers." *Acta Astronautica* 62.10-11 (2008): 556-562.
- [18] Yu, Xinghuo, and Man Zhihong. "Fast terminal sliding-mode control design for nonlinear dynamical systems." *IEEE Transactions on Circuits and Systems I: Fundamental Theory and Applications* 49, no. 2 (2002): 261-264. <https://doi.org/10.1109/81.983876>
- [19] Mobayen, Saleh, and Fairouz Tchier. "Nonsingular fast terminal sliding-mode stabilizer for a class of uncertain nonlinear systems based on disturbance observer." *Scientia Iranica* 24, no. 3 (2017): 1410-1418. <https://dx.doi.org/10.24200/sci.2017.4123>
- [20] Shuang, Li, and Cui Pingyuan. "Landmark tracking based autonomous navigation schemes for landing spacecraft on asteroids." *Acta Astronautica* 62, no. 6-7 (2008): 391-403. <https://doi.org/10.1016/j.actaastro.2007.11.009>
- [21] Furfaro, Roberto, Dario Cersosimo, and Daniel R. Wibben. "Asteroid precision landing via multiple sliding surfaces guidance techniques." *Journal of Guidance, Control, and Dynamics* 36, no. 4 (2013): 1075-1092. <https://doi.org/10.2514/1.58246>
- [22] Gui, Haichao, and Anton HJ de Ruiter. "Control of asteroid-hovering spacecraft with disturbance rejection using position-only measurements." *Journal of Guidance, Control, and Dynamics* 40, no. 10 (2017): 2401-2416. <https://doi.org/10.2514/1.G002617>
- [23] Kasaeian, Seyed Aliakbar, and Masoud Ebrahimi. "Robust Switching Surfaces Sliding Mode Guidance for Terminal Rendezvous in Near Circular Orbit." *Journal of Space Science and Technology* 11, no. 2 (2018): 21-31.
- [24] Perruquetti, Wilfrid, and Jean Pierre Barbot, eds. *Sliding mode control in engineering*. Vol. 11. New York: Marcel Dekker, 2002.
- [25] Azar, Ahmad Taher, and Quanmin Zhu, eds. *Advances and applications in sliding mode control systems*. Cham: Springer International Publishing, 2015.

